Desalination and Water Treatment
www.deswater.com
doi: 10.5004/dwt.2020.25251

183 (2020) 63–72
April

Feasibility study and performance assessment of a new tri-generation integrated system for power, cooling, and freshwater production

Usman Safder[a], Muhammad Akmal Rana[b], ChangKyoo Yoo[a,*]

[a]*Dept. of Environmental Science and Engineering, College of Engineering, Center for Environmental Studies, Kyung Hee University, Seocheon-dong 1, Giheung-gu, Yongin-Si, Gyeonggi-Do, 446-701, Republic of Korea, Tel. +82-31-201-3824; Fax: +82-31-202-8854; email: ckyoo@khu.ac.kr*
[b]*Dept. of Chemical Engineering, COMSATS University Islamabad, Lahore Campus, Lahore, Pakistan*

Received 23 August 2019; Accepted 29 November 2019

ABSTRACT

In the present study, a power, cooling, and freshwater tri-generation system is proposed to meet the global requirements sustainably. A Kalina cycle (KC), an absorption refrigeration cycle (AC), and an organic Rankine cycle (ORC) coupled with reverse osmosis (RO) are integrated to form the proposed system. The performance of the proposed system is analyzed using thermodynamic and economic viewpoint. An integrated system combines the refrigerant loop of the water–ammonia absorption chiller, consisting of an evaporator and throttling valves with KC. The Kalina turbine discharges the heat and combines with generator to loop the ORC and generate power which drives the RO module. A portion of the mass flowrate enters the evaporator to generate cooling after being condensed in the AC unit. The effect of key thermodynamic parameters on system performance is studied using parametric analysis. The results show that the system is capable to generate 1,725 kW of power, 665 kW of cooling, and 3.42 m^3/h of freshwater. The parametric analysis results indicate that the flash tank pressure has an optimum value which should be selected wisely. It is concluded that the parameters related to the KC are dominant ones because they can affect both the KC and the ORC. The proposed system is a flexible adapting power, cooling, and freshwater tri-generation demand.

Keywords: Integrated low-temperature cycles; Parametric analysis; Power, cooling, freshwater tri-generation; Refrigeration; Thermodynamics

1. Introduction

An increase in industrial growth and population highlighted the need of supplying sufficient energy demand and enough freshwater for human activities. In addition, 1% of the world population is dependent on the desalinated water and it is expected 14% of the world population will be encountering water scarcity by 2025 [1]. Energy and water are two critical resources recognized to restrict sustainable development. Utilization of renewable energy sources is considered as a sustainable solution for addressing the energy and freshwater production requirements. Thus, combining renewable energy plants and freshwater production unit is a suitable design for sustainable development [2].

Geothermal energy is one of the renewable energy sources which gained attention due to its benefits to utilize low-grade heat source, a low-temperature cycle, such as Kalina cycle (KC), organic Rankine cycle (ORC), and absorption refrigeration cycle (AC) [3]. KC and ORC are two competitive low-grade heat sources thermodynamic cycles. Many researchers have studied KC and ORC as well as their operation. Ashouri et al. [4] studied a Kalina cycle driven by solar energy to produce power and analyzed the system thermodynamically

* Corresponding author.

Presented at the 12th International Desalination Workshop (IDW2019), 28–30 August 2019, Jeju, Korea

and economically. The authors compared the proposed system with a fuel-driven KC to evaluate the economic effect of solar collectors on the system. The authors concluded that the ammonia mass fraction is the dominant parameter of the cycle and can change performance of the system considerably. Sulaiman et al. [5] studied a hybrid system consisting of solid-oxide fuel cell (SOFC) and an ORC integrated by a single-stage AC. The results showed that tri-generation system's efficiency can be increased by 22%. Patel et al. [6] studied the performance of combined ORC and AC for heating, and cooling production from energy, exergy, and economic viewpoints.

Dozens of papers have focused on the comparison of low-temperature thermodynamic cycles to recover waste heat from systems [7]. Gholamian and Zare [8] investigated KC in comparison with the ORC for waste-heat recovery from SOFC and gas-turbine hybrid system. Shokati et al. [9] performed exergoeconomic comparison between a KC and three types of ORC driven by geothermal energy. The results showed that the KC has the lowest value of unit cost of the power produced. According to a comparison of KC and ORC in the topping cycle, the KC with an ammonia mass fraction can produce 18% more net power and consume 17.8% less electricity [10]. Yogi Goswami [11] proposed a new integrated cycle to produce simultaneous power and cooling using ammonia–water with a single heat source. After that many researchers studied this cycle from different viewpoints. The authors modified the proposed system by rendering the Goswami cycle, which produced a higher quantity of power by superheating the turbine inlet [12,13]. Hasan and Goswami [14] carried out exergy analysis on the Goswami cycle to evaluate its performance. Hadi et al. [15] studied the thermodynamic and thermoeconomic analysis of integrated KC designed only for power and cooling production simultaneously and claimed to obtain thermal efficiency and exergetic efficiency of 20.4% and 16.69%, respectively. Lolos and Rogdakis [16] performed thermodynamic analysis of KC driven by low-temperature heat sources. They only focused on power production and obtained optimum range for the vapor mass fraction on and operating pressures to optimize the performance of the system. Many investigations have been performed to seek the possible position of the Kalina cycle as bottoming or topping cycle and new systems for tri-generation of power, cooling, and heating purposes are considered promising technologies. Li et al. [17] proposed a novel tri-generation system focusing on producing cooling, heating, and power production. They concluded that heating contribution increases the exergy efficiency but with limited cooling capacity. Wang et al. [18] presented a novel system by integration of absorption cooling cycle and KC utilizing low grade heat sources. They also conducted energy and exergy analysis of their proposed cycle and found that increasing the ammonia mass fraction has a vital role in increasing the thermal and exergy efficiencies. The aforementioned cycles are only used to produce cooling, power, and heating only.

Moreover, some regions of the world suffer from severe water stress and the freshwater necessity is expected to expand in the next decades [19]. The various technologies were employed to deal with freshwater scarcity by desalting sea or brackish water. Membrane-based processes, especially reverse osmosis (RO), have been widely used for freshwater production mainly focusing on industrial applications [20]. Among other available technologies, RO has captured great attention because of its low energy and cost requirements and is viable in the areas facing the low availability of fresh water. RO-based freshwater production is 65.5 million m^3/d, which is around 69% of desalinated water production by volume [21]. Seawater RO is expected to play the most important role in future water supplies especially in coastal areas that have not needed it in past years. These include some parts of Europe, South Asia, China, California, and Texas in USA [22]. The use of renewable energy technologies especially photovoltaic and the wind is suitable for providing power to run RO-based plants in remote areas [23]. Few researchers have proposed that hybrid energy systems are suitable for small communities in the mainland. The electricity needed to drive high-pressure pumps in RO is provided by battery storage system coupled with photovoltaic cells and diesel generators are kept for backup for peak hours [24]. The use of fossil fuels to drive the desalination process contributes a lot of pollutants mainly due to the use of diesel generators, contributing to climate change [24]. RO is the most promising desalination technology for the coupling of geothermal power plants in order to produce freshwater and electricity. The various combinations of desalination systems equipped with KC and ORC have been studied. Nafey and Sharaf [25] analyzed the cost rate, energy, and exergy of a combined solar ORC with RO system. They concluded that an ORC is one of the most efficient cycles, which can be used as a mature bottoming cycle to exploit low-grade heat sources and run RO module. Hence, recent research efforts have focused on thermodynamic parametric analysis of KC, comparing the KC with ORC, application of KC and ORC as a bottoming cycle, power, and cooling generation using low-temperature cycles, and integration with desalination unit. However, combining KC with an ORC, refrigeration cycle, and desalination unit to generate power, cooling, and freshwater, simultaneously, as a high efficient system has been rarely done.

In this study to the best of our knowledge, the first to propose a novel tri-generation system consists of low-grade heat source Kalina cycle (KC) to drive an ammonia–water based absorption cooling cycle (AC) integrated with hydrocarbon-based ORC, and desalination unit RO for sustainable production of three useful outputs simultaneously; production of power, generation of process cooling, and freshwater. Concerning the novelty of the proposed tri-generation system, a detailed investigation based on exergy analysis which allows not only quantitative but also qualitative consideration in the energy transformation process is introduced. A parametric study has also been conducted to ascertain the effects of changing the operating variables and fluid thermodynamic properties on the performance parameters of an investigated system.

This paper consists of three major parts. First, the system was modeled thermodynamically to evaluate the performance via thermal and exergetic efficiency. Second, the total annual cost (TAC) of the integrated system was analyzed economically. Third, parametric analysis investigated the effects of the main parameters on the system performance and production costs.

2. Materials and methods

2.1. Tri-generation system configuration

A schematic representation of the proposed system is shown in Fig. 1. The system generates power, cooling, and freshwater based on the functional principles of a Kalina cycle (KC), an organic Rankine cycle (ORC) an absorption refrigeration cycle (AC), and an RO module, respectively. It works in three pressure levels; the lowest (P_{abs}), the intermediate (P_{FT}), and the highest pressure (P_{tur}). The absorber and evaporator operate in the P_{abs} for cooling production and absorbing ammonia–water with different concentrations. The flash tank (FT) under P_{FT} separates the working fluid into two streams with high concentration (state-4), and low concentration (state-13) of ammonia. The hot, high pressure (P_{tur}) stream passes through the KC turbine and generates power. The KC turbine exhaust stream (state-11) after giving fuel to the bottoming ORC, enters the absorber where a basic mass fraction of ammonia is produced by absorbing the weak solution from the flash tank. The high concentration solution (state-4) passed through preheater to preheat the boiler feed solution (state-8) leading to a decreased heat load in the condenser. The absorbed solution (state-1) is then pumped and the cycle is repeated.

In the bottoming cycle, the organic fluid (R245fa) is pumped to the preheater (FTP-2) in which it is heated up to approach its critical temperature by utilizing waste heat of the KC turbine. Then, the organic vapor is expanded in the ORC turbine. A part of the generated power from ORC turbine operates the pump of the RO module. The outflow of the ORC turbine is condensed by exchanging heat with the RO feed water in the ORC condenser (FTP-3).

2.2. Thermodynamic modeling

The thermodynamic properties of all states of the proposed system should be known for any thermodynamic analysis. The models developed by Rashidi et al. [3] and Safder et al. [2] were used considering the following simplifying assumptions.

- The system is under steady-state conditions.
- The heat losses and pressure drops are neglected in pipes and other components.
- The working fluid in the absorber, boiler, condenser, and evaporator outlet of the KC and ORC are saturated.
- The refrigerant is saturated in the condenser and evaporator of the AC.

The energy and mass balance equations of the system's components are summarized in Table 1. The thermodynamic equations of the KC and ORC turbines are given in Eqs. (1) and (2), where $\dot{W}_{turb,KC}$, $\dot{W}_{turb,ORC}$, $\dot{m}_{KC}$, $\dot{m}_{ORC}$, and h are the KC turbine power, ORC turbine power, mass flowrate of the KC turbine, mass flowrate of the ORC turbine, and specific enthalpy, respectively. The power consumption of the pumps ($\dot{W}_{pump}$) is given in Eq. (3), where v is the specific volume of the fluid, η_p is the isentropic efficiency of the pump, $\dot{m}_p$ is the mass flowrate, and P is the pressure [26]. The energy balance equation of the absorber is given in Eq. (4), where $\dot{Q}_{abs}$ is the released heat from the absorber.

The energy balance equations of the heat exchanger (FTP) are presented in Eqs. (5) and (6), where ΔT_{min} represents the temperature difference between the inlet and outlet streams of the cold side. $(T_h)_{in}$ is the temperature of the inlet hot streams, and $(T_c)_{in}$ is the temperature of the inlet cold streams. The boiler and super-heater (SH) are assumed to be operating similar to a heat exchanger unit, where an external hot stream is considered to be a heat source. The required heat can be obtained using Eqs. (7) and (8), respectively. The heat requirement ($\dot{Q}_{FT}$) of the flash tank is obtained using Eqs. (9) and (10), where x is the ammonia mass fraction of fluid. Eqs. (11) and (12) show the simplified energy and mass balance equations of the valves according to the assumed steady-state condition, where $\dot{m}_{valve}$ is the mass flowrate

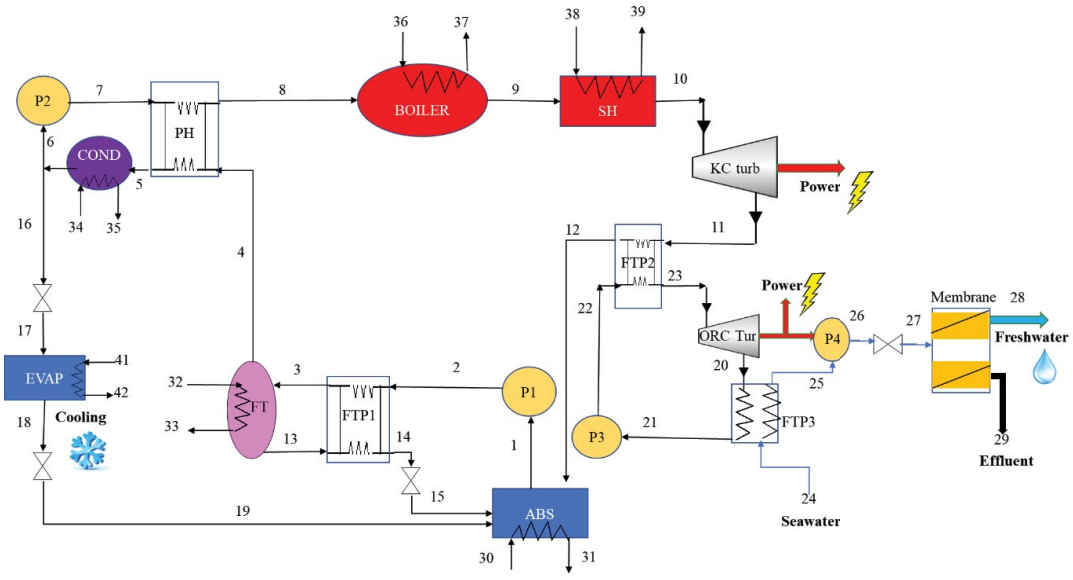

Fig. 1. Schematic representation of the tri-generation system.

Table 1
Thermodynamic model of the KC, ORC, and AC subsystem

Equations	No.
$\dot{W}_{\text{turb,KC}} = \left(\dot{m}_{\text{KC}}\right)\times\left(h_{10}-h_{11}\right)\dot{W}_{\text{turb,KC}} = \left(\dot{m}_{\text{KC}}\right)\times\left(h_{10}-h_{11}\right)$	(1)
$\dot{W}_{\text{turb,ORC}} = \left(\dot{m}_{\text{ORC}}\right)\times\left(h_{23}-h_{20}\right)$	(2)
$\dot{W}_{\text{pump}} = \dfrac{\dot{m}_p \times v \times \left(P_{\text{out}}-P_{\text{in}}\right)}{\eta_p}$	(3)
$\dot{Q}_{\text{abs}} = \dot{m}_{\text{in}} \times h_{\text{in}} - \dot{m}_{\text{out}} \times h_{\text{out}}$	(4)
$\varepsilon_{\text{HEX}} = \dfrac{\Delta T_{\min}}{\left(T_h\right)_{\text{in}} - \left(T_c\right)_{\text{in}}}$	(5)
$SgV = \left(\dot{m}c_p\right)_{\text{cold}} - \left(\dot{m}c_p\right)_{\text{hot}}$	(6)
$\dot{m}_{\text{ext}}\left(h_{36}-h_{37}\right) = \dot{m}_{\text{KC}}\left(h_9-h_8\right)$	(7)
$\dot{m}_{\text{ext}}\left(h_{38}-h_{39}\right) = \dot{m}_{\text{KC}}\left(h_{10}-h_9\right)$	(8)
$\dot{m}_3 \times x_3 = \dot{m}_{13} \times x_{13} + \dot{m}_4 \times x_4$	(9)
$\dot{Q}_{\text{FT}} = \dot{m}_{13} \times h_{13} + \dot{m}_4 \times h_4 - \dot{m}_3 \times h_3$	(10)
$h_{\text{in}} = h_{\text{out}}$	(11)
$(\dot{m}_{\text{valve}})_{\text{in}} = (\dot{m}_{\text{valve}})_{\text{out}}$	(12)

passing through the valves. The subscripts 'in' and 'out' represent inlet and outlet flow.

The RO subsystem is modeled using Eqs. (13) through (25), presented in Table 2. The feed-water mass flowrate ($\dot{m}_f$) is obtained based on the module recovery ratio (RR) and distillate mass flowrate ($\dot{m}_d$), which are given in Eq. (13). The distillate product salt concentration (X_d) is obtained using Eq. (14), where X_f is the feed-water concentration and REJ is the salt rejection ratio. The water content and salinity of the brine stream (X_b) are given in Eqs. (15) and (16), respectively.

The osmotic pressure of the feed (P_f), distillate (P_d), brine streams (P_d), net osmotic pressure membrane ($\Delta\Pi$) is obtained using Eqs. (17) through (20), where $\Delta\Pi_{\text{av}}$ is the average osmotic pressure [27]. The transmembrane pressure (ΔP) is calculated using Eq. (21), where TCF, K_w, $\Delta\Pi$, N_e, N_v, FF, and A_{memb} are temperature correction factor given in Eq. (23), membrane water permeability is given in Eq. (22), net transmembrane osmotic pressure, number of membrane elements, number of pressure vessels, fouling factor and active area of the membrane, respectively.

The required power (HP) of the module pump and specific power consumption (SPC) are, respectively, estimated using Eqs. (24) and (25) where ϱ is the density of the feed water stream and η_{pump} is the pump's isentropic efficiency. The properties of the membrane module constructed by Filmtech with trade name FTSW30HR-380 were used in the current study [2].

Table 2
Governing equations of the RO subsystem

Equations	Units	No.
$\dot{m}_f = \dfrac{\dot{m}_d}{\text{RR}}$	kg/h	(13)
$X_d = X_f \times (1-\text{REJ})$	g/kg	(14)
$\dot{m}_b = \dot{m}_f - \dot{m}_d$	kg/h	(15)
$\dot{m}_f \times X_f = \dot{m}_b \times X_b + \dot{m}_d \times X_d$	g/kg	(16)
$P_f = 75.84 \times X_f$	kPa	(17)
$P_d = 75.84 \times X_d$	kPa	(18)
$P_b = 75.84 \times X_b$	kPa	(19)
$\Delta\Pi = \Delta\Pi_{\text{av}} - P_d$	kPa	(20)
$\Delta P = \left(\dfrac{\dot{m}_d}{3600 \times \text{TCF} \times \text{FF} \times N_e \times N_v \times A_{\text{memb}} \times K_w}\right) + \Delta\Pi$	kPa	(21)
$K_w = \dfrac{\left(6.84/10^8\right)\left(18.6865 - \left(0.177 \times X_b\right)\right)}{\left(T_f + 273\right)}$	L m^{-2} h^{-1} bar^{-1}	(22)
$\text{TCF} = \exp\left(2640\left(\left(\dfrac{1}{298}\right) - \dfrac{1}{\left(273+T_f\right)}\right)\right)$	–	(23)
$\text{HP} = \dfrac{\left(m_f \times \Delta P \times 1{,}000\right)}{\left(3{,}600 \times \rho \times \eta_{\text{pump}}\right)}$	kW	(24)
$\text{SPC} = \dfrac{\text{HP}}{\dot{m}_d}$	kWh/m^3	(25)

All thermal systems could be discussed to their major performance parameters based on the first law of thermodynamics. These parameters are given in Eqs. (26) and (27).

$$\dot{W}_{\text{net}} = \dot{W}_{\text{turb,KC}} + \dot{W}_{\text{turb,ORC}} - \left(\dot{W}_{p1} + \dot{W}_{p2} + \dot{W}_{p3} + \dot{W}_{p4}\right) \tag{26}$$

where $\dot{W}_{\text{net}}$ is the net power of the integrated system. $\dot{W}_{p1}$, $\dot{W}_{p2}$, $\dot{W}_{p3}$, and $\dot{W}_{p4}$ are the power consumption of the pumps 1–4, respectively.

2.3. Economic modeling

The economic modeling of the tri-generation system is developed to assess the TAC. The models reported by Ifaei et al. [28] and Li [29] were used in this section.

The TAC is calculated using Eq. (27).

$$\text{TAC} = \text{AOC} + \text{ACC} \tag{27}$$

where ACC and AOC are the annual capital cost and annual operating cost, respectively. The ACC is obtained by multiplying total capital cost (TCC) by an amortization factor, detailed in reference [30] while AOC is obtained using Eq. (28).

$$\text{AOC} = \text{OM}_l + \text{OM}_i + \text{OM}_p + \text{OM}_{\text{ch}} + \text{OM}_{\text{mem}} \tag{28}$$

$$\text{AF} = \frac{i \times \left((1+i)^{\text{lc}}\right)}{\left((1+i)^{\text{lc}}\right) - 1} \tag{29}$$

where AF and OM are the amortization factor and operating and maintenance cost, respectively. i, lc, and subscripts l, i, p, ch, and mem, represent the interest rate, plant life cycle, labor costs, insurance-maintenance costs, electric power costs, chemical costs, and annual membrane renewal cost, respectively.

All of the costs were updated to a much recent year of 2016 using Eq. (30) and chemical engineering plant index (CI). Required economic constants are presented in Table 3.

$$Z_{k,2016} = Z_{k,2000}\left(\frac{\text{CI}_{2016}}{\text{CI}_{2000}}\right) \tag{30}$$

where $Z_{k,2016}$ is the component cost in 2016, and $Z_{k,2000}$ is the component cost in 2000. CI_{2016} and CI_{2000} are the chemical engineering plant cost indexes in the year 2016 and 2000, respectively [26].

2.4. Exergy analysis

Based on the first and the second law of thermodynamics, the steady-state exergy balance can be expressed as follows [31]:

$$\sum \dot{\text{E}}\text{x}_{\text{in}} + \dot{Q}\left(1 - \frac{T_0}{T}\right) = \sum \dot{\text{E}}\text{x}_{\text{out}} + \dot{W} + \dot{\text{E}}\text{x}_D \tag{31}$$

Table 3
Economic modeling constants

Economic constant	Values
CI_{2016}	541.7
CI_{2000}	394.1
i, %	5
lc, y	20
$Z_{\text{ref, HEX}}$, US$	12,000
lt_{memb}, y	5
CC_{memb}, US$	1,000
lf, y^{-1}	0.85

where subscripts 'in' and 'out' represent inlet and outlet specific exergy to the control volume, respectively. $\dot{\text{E}}\text{x}_D$ is the exergy destruction due to system irreversibilities. The term $\dot{\text{E}}\text{x}$ is given in Eq. (32).

$$\dot{\text{E}}\text{x} = \dot{\text{E}}\text{x}_{\text{ph}} + \dot{\text{E}}\text{x}_{\text{ch}} \tag{32}$$

Where $\dot{\text{E}}\text{x}_{\text{ph}}$ and $\dot{\text{E}}\text{x}_{\text{ch}}$ are the physical and chemical exergies, respectively. The physical and chemical exergy terms are given in Eqs. (33) and (34) [32].

$$\dot{\text{E}}\text{x}_{\text{ph}} = \left(h - h_0\right) - T_0\left(s - s_0\right) \tag{33}$$

$$\dot{\text{E}}\text{x}_{\text{ch}} = \dot{m} \times \left(\frac{\dot{z}_{\text{fluid}}}{\text{MW}_{\text{fluid}}}\right) \times \dot{e}_{\text{ch,fluid}} \tag{34}$$

The $\dot{\text{E}}\text{x}_D$ of each component is calculated using the exergy balance equation between the fuel, product, and components as given in Eq. (35) [28].

$$\dot{\text{E}}\text{x}_{D,k} = \dot{\text{E}}\text{x}_{F,k} - \dot{\text{E}}\text{x}_{P,k} - \dot{\text{E}}\text{x}_{L,k} \tag{35}$$

where $\dot{\text{E}}\text{x}$ represents the exergy rate and the subscripts D, F, P, and L indicate the destruction, fuel, product, and loss streams in the kth components, respectively. The fuel, product, and loss terms of the proposed system are summarized in Table 4. The overall exergy efficiency (η_{ex}) of the system is determined by Eq. (36).

$$\eta_{\text{ex}} = \frac{\dot{\text{E}}\text{x}_{28} + \dot{W}_{\text{turb,KC}} + \dot{W}_{\text{turb,ORC}}}{Q_{\text{in}}\left(1 - \left(\frac{T_0}{T_{31}} + 273\right)\right)} \tag{36}$$

where T_0 represents the dead state temperature in Celsius degrees. The dead state is assumed to be the air that rests at 25°C and 1 bar.

3. Results and discussion

3.1. System performance

The energy, cost, and exergy analyses were conducted to determine the energy efficiency, performance, generated

cooling, freshwater production, TAC, exergetic efficiency, and exergy destruction of the tri-generation system.

The energetic performance of the proposed tri-generation system was obtained using the thermodynamic properties and the energetic model presented in Eqs. (1) through (26). The energy analysis results of current reported system and comparison with studies performed by Zheng et al. [33], Rashidi et al. [3] and El-Syed et al. [34] are summarized in Table 5. It is evident from the table that operating the absorber at 1 bar pressure and slightly increasing the turbine inlet temperature the authors were able to achieve higher net power output of 1,725 kW, higher cooling capacity of 665 kW with additional 3.42 m^3/h of freshwater. It is also noticeable that the power generated by the Kalina turbine is far higher than the generated power by the ORC turbine. This is because both pressure ratio and mass flow rate of the Kalina turbine are higher. On the other hand, 8.37 kW power is consumed by RO pump to produce 3.42 m^3/h freshwater. The seawater enters in RO module in high temperature to have better performance. In addition, the cooling and heating capacity of the tri-generation system is 665 and 6,381 kW, respectively.

As can be seen, heating capacity is almost 9.5 times as the cooling capacity. This is because water before going to the boiler and super-heater is heated in the pre-heater and condenser, as a result from its temperature increase. This pre-heating effect increases mass flow rate of hot solution and consequently heating capacity of the investigated system increases considerably. In general, net output power of the tri-generation system is equal to 1,725 kW, and TAC of the system is 7.29×10^5 \$/y.

Abkari et al. [35] reported a combined cogeneration system for the production of electric power and freshwater using Kalina cycle and their reported thermal efficiency was ranging between 16% and 18.2% but current reported system is 19.35% energy efficient with additional product of cooling and same amount of freshwater production. To have a better insight into the performance of the proposed system, exergy analysis was performed using thermodynamic properties and definitions for fuel and product presented in Eqs. (31)–(36), and Table 4. The exergetic efficiency of the tri-generation is equal to 23.35%. Fig. 2 presents the exergy destruction of components in the tri-generation system. As can be seen, the condenser (COND) exhibited the highest

Table 4
Fuel-product definition of the tri-generation system components

Component	Fuel	Product	Loss
Boiler	$(Ex_{36}–Ex_{37}) \times \dot{m}_{ext}$	$(Ex_9–Ex_8) \times \dot{m}_8$	–
SH	$(Ex_{38}–Ex_{39}) \times \dot{m}_{ext}$	$(Ex_{10}–Ex_9) \times \dot{m}_9$	–
Kalina turbine	$(Ex_{11}–Ex_{10}) \times \dot{m}_{11}$	$\dot{W}_{turb,KC}$	–
FTP1	$(Ex_3–Ex_2) \times \dot{m}_4$	$(Ex_{13}–Ex_{14}) \times \dot{m}_{14}$	–
Absorber	$Ex_{15}\dot{m}_{15} + Ex_{19}\dot{m}_{19} + Ex_{12}\dot{m}_{12}–Ex_1\dot{m}_1$	$(Ex_{31}–Ex_{30}) \times \dot{m}_{31}$	–
Pump 1	$\dot{W}_{p1}$	$(Ex_2–Ex_1) \times \dot{m}_1$	–
Pump 2	$\dot{W}_{p2}$	$(Ex_7–Ex_6) \times \dot{m}_6$	–
Pump 3	$\dot{W}_{p3}$	$(Ex_{22}–Ex_{21}) \times \dot{m}\dot{m}_{ORC}$	–
PH	$(Ex_4–Ex_5) \times \dot{m}_4$	$(Ex_8–Ex_7) \times \dot{m}_7$	–
Evap	$(Ex_{16}–Ex_{18}) \times \dot{m}_{16}$	$(Ex_{42}–Ex_{41}) \times \dot{m}_{42}$	–
FTP2	$(Ex_{11}–Ex_{12}) \times \dot{m}_{11}$	$(Ex_{23}–Ex_{22}) \times \dot{m}_{ORC}$	–
ORC turbine	$(Ex_{23}–Ex_{20}) \times \dot{m}_{ORC}$	$\dot{W}_{turb,ORC}$	–
FTP3	$(Ex_{20}–Ex_{21}) \times \dot{m}_{ORC}$	$(Ex_{25}–Ex_{24}) \times \dot{m}_f$	–
Pump 4	$\dot{W}_{p4}$	$(Ex_{26}–Ex_{25}) \times \dot{m}_d$	–
RO membrane	$Ex_{26} \times \dot{m}_f$	$Ex_{28} \times \dot{m}_d$	$Ex_{29} \times \dot{m}_b$

Table 5
Performance indicators of the system and comparison with reported studies

Parameters	Current study	Ref. [31]	Ref. [3]	Ref. [32]
Absorber pressure, bar	1.0	0.981	1.7	1.7
Turbine inlet temperature, °C	380	350	280	510
Net power output, kW	1,725	747.7	1,550	1,722
Cooling capacity, kW	665	298	277	–
Power consumed by RO, kW	8.37	–	–	–
Freshwater production, m^3/h	3.42	–	–	–
Energy efficiency, %	19.35	24	15.2	16.1
Total annual cost, \$/yr	7.29×10^5	–	5.62×10^6	6.11×10^6

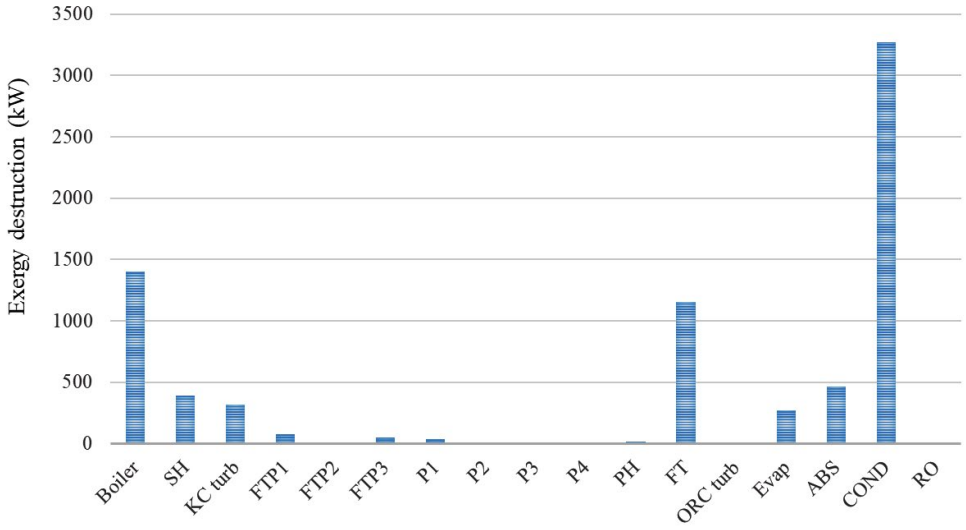

Fig. 2. Exergy destruction of each component.

rate of exergy destruction and it is responsible for 46% of total exergy destruction. This is because of high temperature difference between hot and cold streams. The boiler and flash tank, two other exergy destruction components ranked second and third after COND with nearly 1,399 and 1,151 kW exergy destruction, respectively. The absorber (ABS), super-heater (SH), and evaporator (EVAP) could be attributed to 6.5%, 5.5%, and 3.8%, respectively, of the total fuel exergy. All the other components have a lower share in total exergy destruction of the system.

Fig. 3 compares the total energetic and exergetic efficiency of the tri-generation system with some literature. As can be seen, the power-cooling system studied by Rashidi et al. [3], and Rashidi and Yoo [32], and stand-alone Kalina cycle in ref. [3] achieved 18.8%, and 16.1% of energetic efficiency, while 12.32%, and 11.53% of exergetic efficiency, respectively. At the same time, the power and refrigeration cycle which analyzed by Hasan et al. [36] has an energetic efficiency of around 12.3%. At the same ammonia mass fraction, the energetic and exergetic efficiency, respectively, are around 19.35%, and 23.35%, which are much higher compared with literature study. Comparison of literature result with this study shows that performance of integrated KC, ORC, AC, and RO system is higher than most of the other proposed multi-generation systems, which are based on Kalina cycle using ammonia–water mixture as a working fluid.

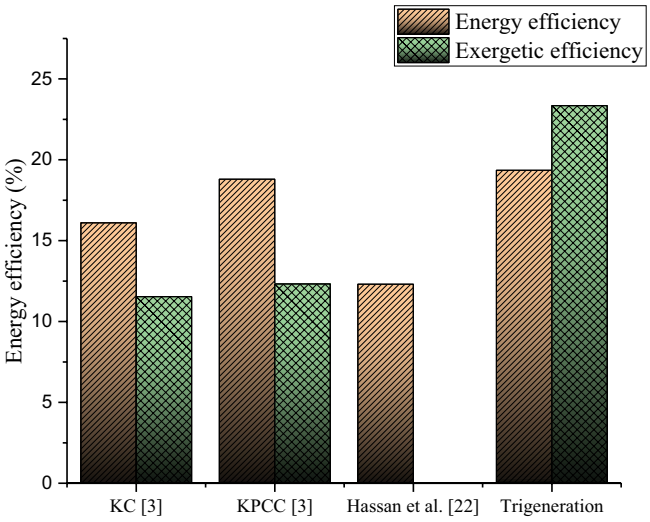

Fig. 3. Thermodynamic comparison of the proposed system.

3.2. Parametric analysis

In this section, the effect of the key thermodynamic parameters on the system performance is examined. These parameters are flash pressure, absorber pressure, ammonia mass fraction of basic solution, and salinity of RO system feed water.

3.2.1. Effect of flash tank pressure on the system performance

Fig. 4a shows the effect of the flash pressure on the total exergy destruction and efficiency of the system. As can be seen, there is an optimum value for both exergetic efficiency and exergy destruction of the system, but the optimum value is different for these two indicators. While exergy efficiency of the system maximizes in flash pressure equal to 434 kPa, the total exergy destruction of the system minimizes in 510 kPa.

Fig. 4b is presented to realize why there is an optimum value for exergy analysis. When flash pressure increases, it affects the generated power and cooling capacity in various ways. First, the mass flow rate of produced mixture is reduced, which increases pressure ratio of the turbine. By this, generated power by KC turbine increases first but then the effect of mass flow rate dominates and generated power of turbine decreases. When flash temperature increases, its outlet temperature increases too. As a result, cooling generation by the evaporator decreases. In addition, increasing the flash tank pressure leads to lower total cost with some small ups and downs.

3.2.2. Effect of absorber pressure on the system performance

Fig. 5 shows the performance variation of the system with changes in the absorber pressure. As can be seen in Fig. 5a, by changing absorber pressure from 100 to 200 kP, exergetic efficiency goes down to reach the minimum point of 20.08% at 200 kPa. Meanwhile, total exergy destruction decreases with constant slope. Furthermore, when this parameter increases, net power generated by the system and cooling production decreases which decreases the exergetic efficiency of the system, as shown in Fig. 5b. As the load on the condenser decreases, which reduces the total exergy destruction of the system, and TAC of the system decreases.

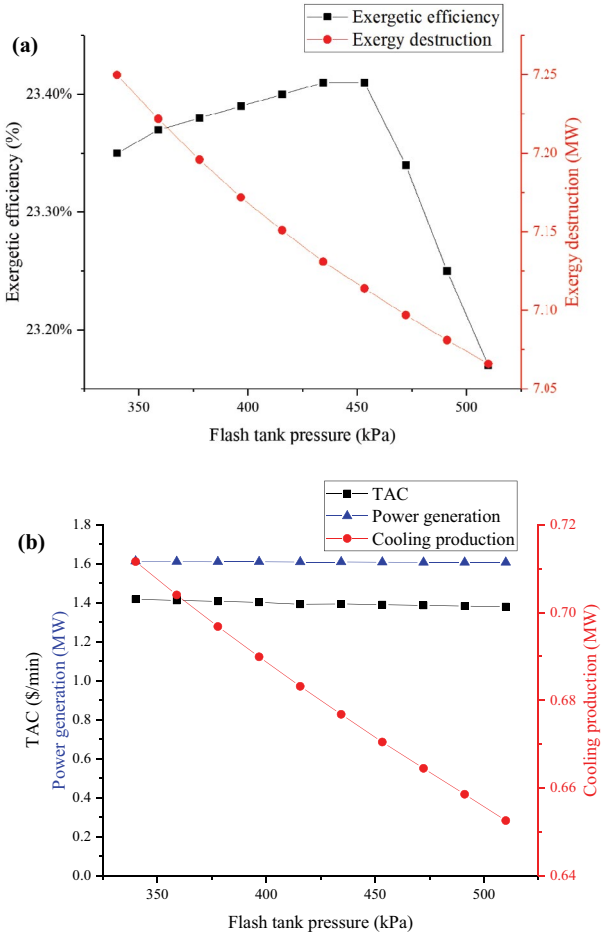

Fig. 4. Effect of the flash tank pressure on (a) exergetic analysis and (b) performance analysis.

3.2.3. Effect of ammonia mass fraction of basic solution

Fig. 6 represents the effect of ammonia mass fraction of basic solution on total system performance. As can be seen in Fig. 6, increasing ammonia mass fraction from 70% to 80% can affect the exergetic efficiency, rate of exergy destruction, TAC, cooling production, and net generated power of the system. According to Fig. 6a, the exergetic efficiency increases gradually to reach the peak point, 24.98%, at 80% of ammonia mass fraction, while total exergy destruction increases gradually. This is because when ammonia mass fraction increases, mass flow rate of produced ammonia–water in heat exchanger decreases. On the other hand, the mass flow rate of stream 41 increases, which itself results in higher cooling generation in the evaporator, while net generated power by the system decreases, as shown in Fig. 6b. Totally, increase in refrigeration production dominates and leads to increase in exergy efficiency of the system.

3.2.4. Effect of RO system feed water salinity

Fig. 7 shows the effects of feed water salinity on the performance of the RO subsystem. The increasing salinity of the feed water from 30,000 ppm to 65,000 ppm, leads to slightly higher production of freshwater. It increases power consumed by RO subsystem, which results in an increment in SPC of the RO unit, while total exergy destruction of the tri-generation system remains constant.

4. Conclusion

In this study, an integrated Kalina cycle (KC) with absorption refrigeration cycle (AC) is used to produce cooling and

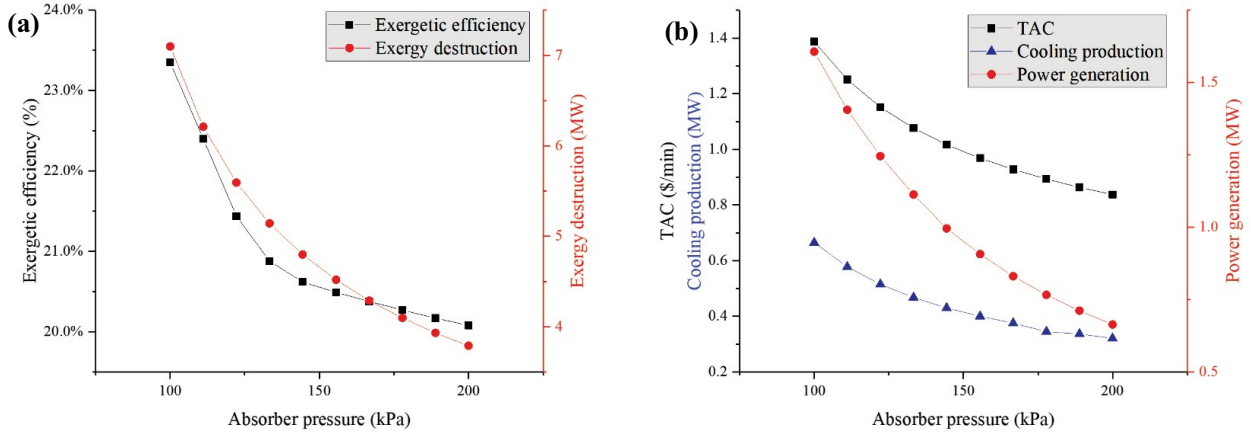

Fig. 5. Effect of the absorber pressure on (a) exergy analysis, and (b) cooling capacity, power generation, and TAC.

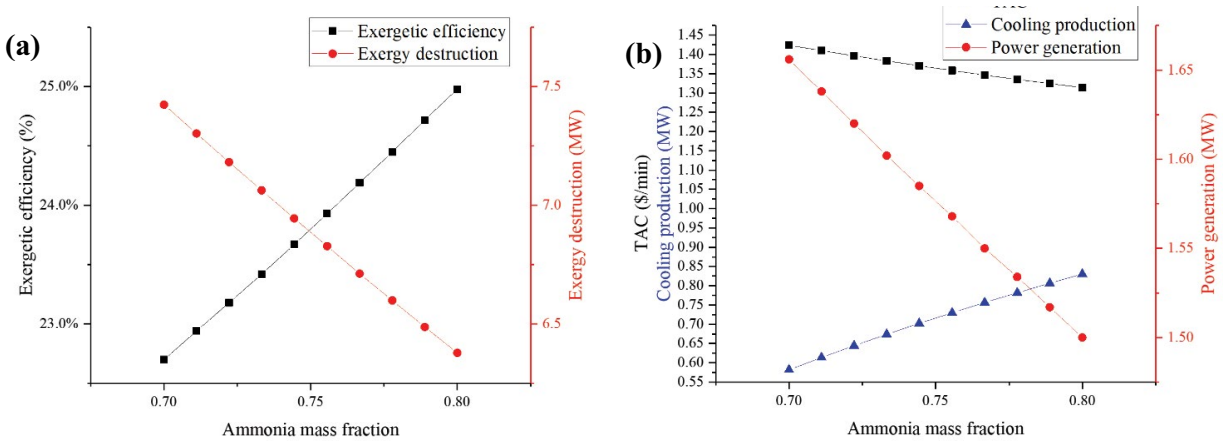

Fig. 6 Effect of ammonia mass fraction of basic solution on total system performance by (a) exergy analysis and (b) cooling capacity, power generation, and TAC.

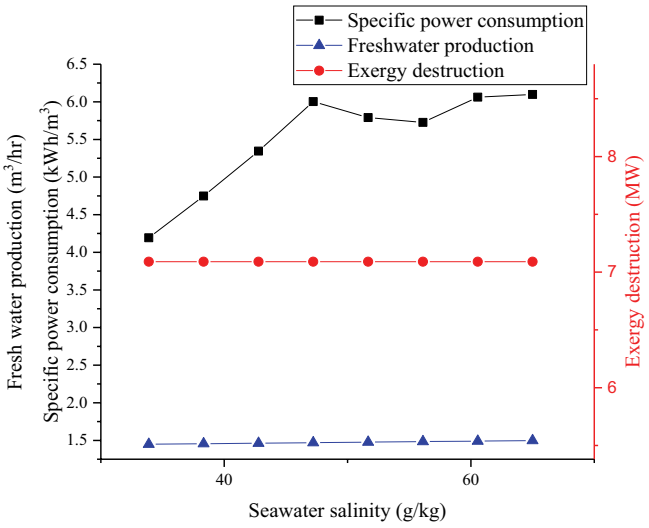

Fig. 7. Effect of feed water salinity on total system performance.

power. An ORC and an RO unit is integrated to the cycle to increase generated power and freshwater. The main contributions of this work are defined as follows:

- Designing a new combination of KC with ORC, AC, and RO for simultaneously power, cooling, and freshwater generation.
- Using low-temperature heat source as the driving energy.
- Comprehensive analysis of the proposed system from the energy, economic, and exergy viewpoints.
- Through parametric analysis of the key metrics effect on the proposed system.

The most important conclusion of the study is summarized as follows:

- The proposed system has the capacity to produce 1,725 kW power, 665 kW of refrigeration load, and 3.42 m^3/h of freshwater with exergetic efficiency of 23.35%. The condenser has contributed almost 46% of total exergy destruction on system performance.
- Flash tank pressure has a parameter which has an optimum value, while the other parameters affect the system linearly. Therefore, best value of this parameter should be selected to achieve the best performance of the investigated system. It can boost the exergetic efficiency of the system up to 0.8%.
- The effect of parameters which are related to Kalina cycle is higher than parameters related to ORC. This is because more than 90% of total output power of the system generates in Kalina turbine. Moreover, any changes in parameters of Kalina cycle somehow changes the performance of the ORC by changing mass flow rate of produced ammonia–water mixture in the heat exchanger.

Acknowledgments

This work was supported by the National Research Foundation (NRF) grant funded by the Korean government (MSIT) (No. NRF-2017R1E1A1A03070713), and Korea Ministry of Environment (MOE) as Graduate School specialized in Climate Change.

References

[1] D. Seckler, R. Barker, U. Amarasinghe, Water scarcity in the twenty-first century, Int. J. Water Resour. Dev., 15 (1999) 29–42.
[2] U. Safder, P. Ifaei, C. Yoo. Multi-objective optimization and flexibility analysis of a cogeneration system using thermorisk and thermoeconomic analyses, Energy Convers. Manage., 166 (2018) 602–636.
[3] J. Rashidi, P. Ifaei, I.J. Esfahani, A. Ataei, C.K. Yoo, Thermodynamic and economic studies of two new high efficient power-cooling cogeneration systems based on Kalina and absorption refrigeration cycles, Energy Convers. Manage., 127 (2016) 170–186.
[4] M. Ashouri, A.M. Khoshkar Vandani, M. Mehrpooya, M.H. Ahmadi, A. Abdollahpour, Techno-economic assessment of a Kalina cycle driven by a parabolic Trough solar collector, Energy Convers. Manage., 105 (2015) 1328–1339.
[5] F.A. Al-Sulaiman, I. Dincer, F. Hamdullahpur, Energy analysis of a trigeneration plant based on solid oxide fuel cell and Rankine cycle, Int. J. Hydrogen Energy, 35 (2010) 5104–5113.

[6] B. Patel, N.B. Desai, S.S. Kachhwaha, V. Jain, N. Hadia, Thermo-economic analysis of a novel organic Rankine cycle integrated cascaded vapor compression–absorption system, J. Clean. Prod., 154 (2017) 26–40.
[7] U. Safder, P. Ifaei, C. Yoo, Multi-scale smart management of integrated energy systems, Part 2: Weighted multi-objective optimization, multi-criteria decision making, and multi-scale management (3M) methodology, Energy Convers. Manage., 198 (2019) 111830.
[8] E. Gholamian, V. Zare, A comparative thermodynamic investigation with environmental analysis of SOFC waste heat to power conversion employing Kalina and Organic Rankine Cycles, Energy Convers. Manage., 117 (2016) 150–161.
[9] N. Shokati, F. Ranjbar, M. Yari, Exergoeconomic analysis and optimization of basic, dual-pressure and dual-fluid ORCs and Kalina geothermal power plants: a comparative study, Renew. Energy, 83 (2015) 527–542.
[10] C.E. Campos Rodríguez, J.C. Escobar Palacio, O.J. Venturini, E.E. Silva Lora, V.M. Cobas, D. Marques Dos Santos, F.R. Lofrano Dotto, V. Gialluca, Exergetic and economic comparison of ORC and Kalina cycle for low temperature enhanced geothermal system in Brazil, Appl. Therm. Eng., 52 (2013) 109–119.
[11] D. Yogi Goswami, Solar Thermal power technology: present status and ideas for the future, Energy Sources, 20 (1998) 137–145.
[12] J. Wang, Y. Dai, L. Gao. Parametric analysis and optimization for a combined power and refrigeration cycle, Appl. Energy, 85 (2008) 1071–1085.
[13] X. Jing, D. Zheng, Effect of cycle coupling-configuration on energy cascade utilization for a new power and cooling cogeneration cycle, Energy Convers. Manage., 78 (2014) 58–64.
[14] A.A. Hasan, D.Y. Goswami, Exergy analysis of a combined power and refrigeration thermodynamic cycle driven by a solar heat source, J. Sol, Energy Eng., 125 (2003) 55–60.
[15] H. Ghaebi, T. Parikhani, H. Rostamzadeh, B. Farhang, Thermodynamic and thermoeconomic analysis and optimization of a novel combined cooling and power (CCP) cycle by integrating of ejector refrigeration and Kalina cycles, Energy, 139 (2017) 262–276.
[16] P.A. Lolos, E.D. Rogdakis, A Kalina power cycle driven by renewable energy sources, Energy, 34 (2009) 457–464.
[17] R. Li, H. Wang, E. Yao, S. Zhang, Thermo-economic comparison and parametric optimizations among two compressed air energy storage system based on kalina cycle and ORC, Energies, 10 (2017) 1–9.
[18] J. Wang, J. Wang, P. Zhao, Y. Dai, Thermodynamic analysis of a new combined cooling and power system using ammonia-water mixture, Energy Convers. Manage., 117 (2016) 335–342.
[19] R. Abell, K. Vigerstol, J. Higgins, S. Kang, N. Karres, B. Lehner, A. Sridhar, E. Chapin, Freshwater biodiversity conservation through source water protection: quantifying the potential and addressing the challenges, Aquat. Conserv. Mar. Freshwater Ecosyst., 29 (2019) 1022–1038.
[20] U. Safder, P. Ifaei, K. Nam, J. Rashidi, C. Yoo, Availability and reliability analysis of integrated reverse osmosis - forward osmosis desalination network, Desal. Wat. Treat., 109 (2018) 1–7.
[21] E. Jones, M. Qadir, M.T.H. van Vliet, V. Smakhtin, Kang S mu, The state of desalination and brine production: a global outlook, Sci. Total Environ., 657 (2019) 1343–1356.
[22] G. Amy, N. Ghaffour, Z. Li, L. Francis, R.V. Linares, T. Missimer, S. Lattemann, Membrane-based seawater desalination: present and future prospects, Desalination, 401 (2017) 16–21.
[23] C. Koroneos, A. Dompros, G. Roumbas, Renewable energy driven desalination systems modelling, J. Clean. Prod., 15 (2007) 449–464.
[24] B. Wu, A. Maleki, F. Pourfayaz, M.A. Rosen, Optimal design of stand-alone reverse osmosis desalination driven by a photovoltaic and diesel generator hybrid system, Sol. Energy, 163 (2018) 91–103.
[25] A.S. Nafey, M.A. Sharaf, Combined solar organic Rankine cycle with reverse osmosis desalination process: energy, exergy, and cost evaluations, Renew Energy, 35 (2010) 2571–2580.
[26] P. Ifaei, J. Rashidi, C.K. Yoo, Thermoeconomic and environmental analyses of a low water consumption combined steam power plant and refrigeration chillers – Part 1: Energy and economic modelling and analysis, Energy Convers. Manage., 123 (2016) 610–624.
[27] Fundamentals of Salt Water Desalination, 2002.
[28] P. Ifaei, U. Safder, C. Yoo, Multi-scale smart management of integrated energy systems, Part 1: Energy, economic, environmental, exergy, risk (4ER) and water-exergy nexus analyses, Energy Convers. Manage., 197 (2019) 111851.
[29] G. Li, Organic Rankine cycle performance evaluation and thermoeconomic assessment with various applications part II: economic assessment aspect, Renew. Sustain. Energy Rev., 64 (2016) 490–505.
[30] H.T. Nguyen, U. Safder, X.Q. Nhu Nguyen, C. Yoo, Multi-objective decision-making and optimal sizing of a hybrid renewable energy system to meet the dynamic energy demands of a wastewater treatment plant, Energy, (2019) 116570. doi:10.1016/J.ENERGY.2019.116570.
[31] I. Janghorban Esfahani, C.K. Yoo, Exergy analysis and parametric optimization of three power and fresh water cogeneration systems using refrigeration chillers, Energy, 69 (2013) 340–355.
[32] J. Rashidi, C.K. Yoo, Exergetic and exergoeconomic studies of two highly efficient power-cooling cogeneration systems based on the Kalina and absorption refrigeration cycles, Appl. Therm. Eng., 124 (2017) 1023–1037.
[33] D. Zheng, B. Chen, Y. Qi, H. Jin, Thermodynamic analysis of a novel absorption power/cooling combined-cycle, Appl. Energy, 83 (2006) 311–323.
[34] T.M. El-Sayed, Y. El-Sayed, M. Tribus, A Theoretical Comparison of the Rankine and Kalina Cycles, Proc. Analysis of Energy Systems, Design and Operation, Presented at the Winter Annual Meeting of the American Society of Mechanical Engineers, Miami Beach, Florida, 1985, p. 97.
[35] M. Akbari, S.M.S. Mahmoudi, M. Yari, M.A. Rosen, Energy and exergy analyses of a new combined cycle for producing electricity and desalinated water using geothermal energy, Sustainability, 6 (2014) 1796–1820.
[36] A.A. Hasan, D.Y. Goswami, S. Vijayaraghavan, First and second law analysis of a new power and refrigeration thermodynamic cycle using a solar heat source, Sol. Energy, 73 (2002) 385–393.